Saudi Journal of Biological Sciences (2017) **24**, 1355–1360

King Saud University

Saudi Journal of Biological Sciences

www.ksu.edu.sa
www.sciencedirect.com

ORIGINAL ARTICLE

Adsorption characteristics of sulfur solution by acticarbon against drinking-water toxicosis

Shengbo Ge [a], Zhenling Liu [b], Yuzo Furuta [c], Wanxi Peng [a,c,*]

[a] *School of Materials Science and Engineering, Central South University of Forestry and Technology, Changsha 410004, China*
[b] *School of Management, Henan University of Technology, Zhengzhou, Henan 450001, China*
[c] *Laboratory of Biomaterials Science, Kyoto Prefectural University, Kyoto, Japan*

Received 28 June 2016; revised 1 September 2016; accepted 2 September 2016
Available online 9 September 2016

KEYWORDS

Acticarbon;
Drinking-water toxicosis;
$Fe_2(SO_4)_3$;
$Na_2S_2O_8$;
Na_2SO_3

Abstract Sulfur and ammonia nitrogen are rich nutrient pollutants, after entering water can cause algal blooms, cause eutrophication of water body, the spread of them will not only pollute the environment, destroy the ecological balance, but also harm human health through food chain channels, especially drinking-water toxicosis. Acticarbon can adsorb harmful substances, it was beneficial for people's health. In order to figure out the optimal adsorption condition and the intrinsic change of acticarbon, five chemicals were adsorbed by acticarbon and analyzed by FT-IR. The optimal adsorption condition of $Fe_2(SO_4)_3$, Na_2SO_4, $Na_2S_2O_8$, S and Na_2SO_3 was 9 g/1000 g at 80 min, 21 g/1000 g at 20 min, 15g/1000 g at 20 min, 21 g/1000 g at 60 min and 21 g/1000 g at 100 min, respectively. FT-IR spectra showed that acticarbon had eight characteristic peaks, such as S-S stretch, H_2O stretch, O—H stretch, —C—H stretch, C=O or C=C stretch, CH_2 bend, C—H were at 3850 cm^{-1}, 3740 cm^{-1}, 3435 cm^{-1}, 2925 cm^{-1}, 1630 cm^{-1}, 1390 cm^{-1}, 1115 cm^{-1}, 600 cm^{-1}, respectively. For FT-IR spectra of $Fe_2(SO_4)_3$, the peaks at 3850 cm^{-1}, 3740 cm^{-1}, 2925 cm^{-1} achieved the maximum with 9 g/1000 g at 20 min. For Na_2SO_4, the peaks at 2925 cm^{-1}, 1630 cm^{-1}, 1390 cm^{-1}, 1115 cm^{-1}, 600 cm^{-1} achieved the maximum with 21 g/1000 g at 120 min. For ones of $Na_2S_2O_8$, the peaks at 3850 cm^{-1}, 3740 cm^{-1}, 1390 cm^{-1}, 1115 cm^{-1}, 600 cm^{-1}, achieved the maximum with 2 g/1000 g at 80 min. For ones of S, the peaks at 3850 cm^{-1}, 3740 cm^{-1}, 2925 cm^{-1} achieved the maximum with 19 g/1000 g at 100 min, the peaks at 1390 cm^{-1}, 1115 cm^{-1}, 600 cm^{-1} achieved the maximum with 19 g/1000 g at 20 min. For FT-IR spectra of Na_2SO_3, the peaks at 1630 cm^{-1}, 1390 cm^{-1}, 1115 cm^{-1}, 600 cm^{-1} achieved the maximum with 2 g/1000 g at 100 min. It provided that acticarbon could adsorb and desulphurize from sulfur solution against drinking-water toxicosis.

* Corresponding author at: School of Materials Science and Engineering, Central South University of Forestry and Technology, Changsha 410004, China.
E-mail address: pengwanxi@163.com (W. Peng).

Peer review under responsibility of King Saud University.

ELSEVIER Production and hosting by Elsevier

http://dx.doi.org/10.1016/j.sjbs.2016.09.010

1. Introduction

Sulfur and ammonia nitrogen mainly come from chemical fertilizers, processed meat, leather and other industry emissions of industrial waste water, and city life sewage and farmland irrigation and drainage (He et al., 2008; Mao et al., 2000; Chai et al., 2010). Sulfur and ammonia nitrogen are rich nutrient pollutants, after entering water can cause algal blooms, cause eutrophication of water body, the spread of them will not only pollute the environment, destroy the ecological balance, but also harm human health through food chain channels, such as drinking-water toxicosis. Ecological effects of acid precipitation can be determined from the timing of changes in lake chemistry or acid-sensitive micro fossils and metallic pollutants in sediments. This is thought to be a result of a few factors: increased construction of large power plants and smelters with tall smokestacks coupled with a decrease in use of coal for home heating, converting the local air pollution problem into along-range, transboundary one; emissions of NO_x and other pollutants that aid in the oxidation of sulfur and nitrogen oxide have increased; and it took years for lakes, streams and their catchments to lose their buffering capabilities, so that lower pH levels were not recognized until sometime after the precipitation became acidic. Anthropogenic emissions are comparable to natural emissions on the global level, but regionally over 90% of sulfur deposited from the atmosphere is anthropogenic (Schindler, 1988).

Acticarbon can use almost any type of carbon materials, such as wood (Wang et al., 2009a), sawdust (Zhang et al., 2010), coal (Ahmadpour and Do, 1996), shells (Chandra et al., 2009), the stone of the fruit (Jumasiah et al., 2005), bagasse, oil waste, waste plastics (Zhou et al., 2007), paper and leather scrap (Yuan et al., 2004), waste tires and urban waste (Wang, 2004). Acticarbon with highly developed porous structure and huge specific surface area (Ding et al., 2002), good chemical stability and thermal stability, high mechanical strength and surface contains a variety of oxygen containing functional groups (Yu et al., 2005 and Pu and Jiang, 2005). What's more, acticarbon, which contained potassium, calcium and other minerals, could have adsorption and filtration of extractives, oil, other matters (Peng et al., 2013a,b,c, 2014a, 2012, 2011; Xiao et al., 2013; Wang et al., 2013; Peng and Le, 2012; Liu et al., 2008; Zhang et al., 2008; Qi et al., 2012). The fabric inhibited bacterial metabolism causing fewer allergic skin reactions than other fibers sterilized with antimicrobial agents. Because the trait was due to the highly porous structure of the bamboo fabric, it could absorb sulfur-based compounds, nitrogen-based compounds and so on (Milena et al., 2003; Ikuo et al., 2001; Masakazu et al., 2003; Kei et al., 1994; Wang et al., 2006; Xue et al., 2014; Cui et al., 2014). In order to figure out the optimal adsorption condition and the intrinsic change of the acticarbon, five chemicals were adsorbed by acticarbon and were analyzed by FT-IR.

2. Materials and methods

2.1. Materials

Acticarbon, $Fe_2(SO_4)_3$, Na_2SO_4, $Na_2S_2O_8$, S, and Na_2SO_3 were purchased from the market.

2.2. Methods

The $Fe_2(SO_4)_3$ powder was weighed in quantities of 5 g, 9 g, and 21 g . These powder and 4 g over dry acticarbon were put into beaker which equipped with 1000 ml water, respectively.It was stirred in a beaker for 20 min, 80 min and 120 min. The Na_2SO_4 powder was weighed in quantities of 11 g, 19 g, and 21 g. These powder and 4 g over dry acticarbon were put into beaker which equipped with 1000 ml water, respectively. It was stirred in a beaker for 20 min, 60 min and 120 min, respectively. The $Na_2S_2O_8$ powder was weighed

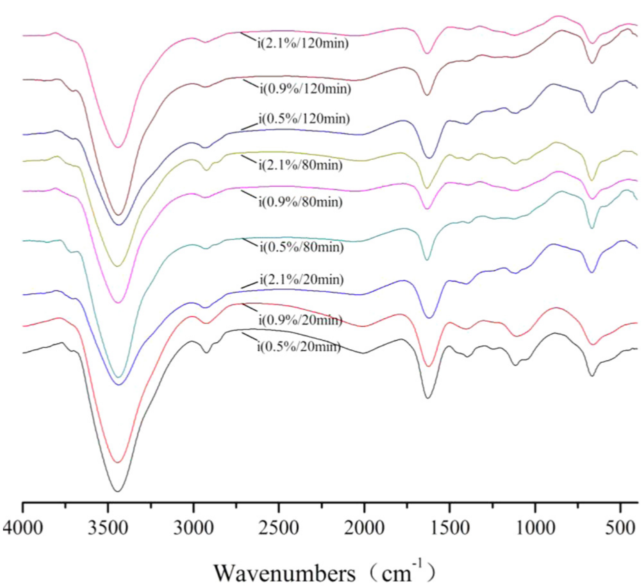

Figure 1 FT-IR spectra of acticarbon during adsorption of $Fe_2(SO_4)_3$ solution.

Table 1 Adsorption results.

SC (%)	$Fe_2(SO_4)_3$ Stir time (min)			SC (%)	Na_2SO_4 Stir time (min)			SC (%)	$Na_2S_2O_8$ Stir time (min)			SC (%)	S Stir time (min)			SC (%)	Na_2SO_3 Stir time (min)		
	20	80	120		20	60	120		20	80	100		20	60	100		20	40	100
0.5	3.76	2.49	1	1.1	1.25	0.75	2.51	0.2	0.5	1.79	1.03	0.2	7.75	4.52	4.73	0.2	0	2.74	1.75
0.9	1.75	23.7	0.5	1.9	3.52	1.99	2.26	1.1	8.25	3.23	2.23	1.9	37.3	58.6	11.5	1.1	2.74	2.74	2.26
2.1	17.5	18.5	2.75	2.1	8.21	1.75	2.99	1.5	20.1	12.7	2.19	2.1	37.7	80.3	32.8	2.1	1.25	2.26	4.26

Note: SC – Concentration of sulfur solution.

in quantities of 2 g, 11 g, and 15 g. These powder and 4 g over dry acticarbon were put into beaker which equipped with 1000 ml water, respectively. It was stirred in a beaker for 20 min, 80 min and 100 min. The S powder was weighed in quantities of 2 g, 19 g, 21 g. These powder and 4 g over dry acticarbon were put into beaker which equipped with 1000 ml water, respectively. It was stirred in a beaker for 20 min, 60 min and 100 min. The Na_2SO_3 powder was weighed in quantities of 2 g, 11 g, 21 g. These powders and 4 g over dry acticarbon were put into a beaker which contained 1000 ml water. It was stirred in a beaker for 20 min, 40 min and 100 min. Each acticarbon was removed, dried, and weighed.

FT-IR spectra. FT-IR spectra of the above samples were obtained using a Thermo Scientific Nicolet iN10 FT-IR microscope as previously (Lin et al., 2015; Peng et al., 2014b, 2015; Sun et al., 2014; Wang et al., 2009b; Parag and Bhanu, 2013).

3. Results and analysis

Based on the above test, the results of adsorption were obtained and listed in Table 1.

3.1. SC Effect

Based on Table 1, when the concentrations of $Fe_2(SO_4)_3$ were 5 g/1000 g, 9 g/1000 g, 21 g/1000 g, $Fe_2(SO_4)_3$'s adsorption

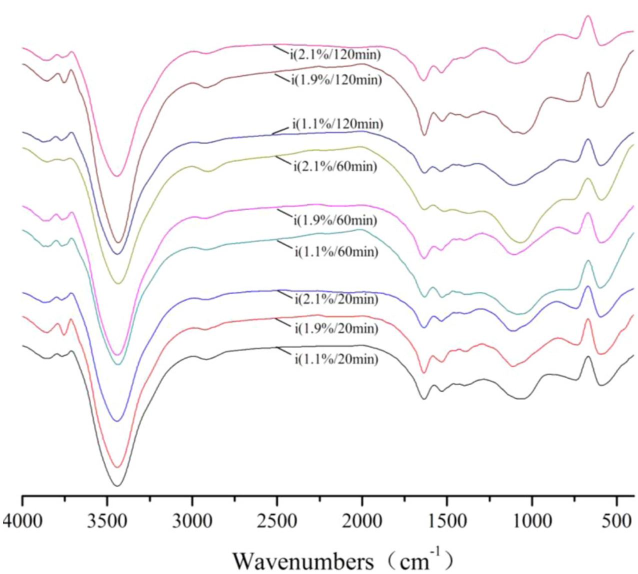

Figure 2 FT-IR spectra of acticarbon during adsorption of Na_2SO_4 solution.

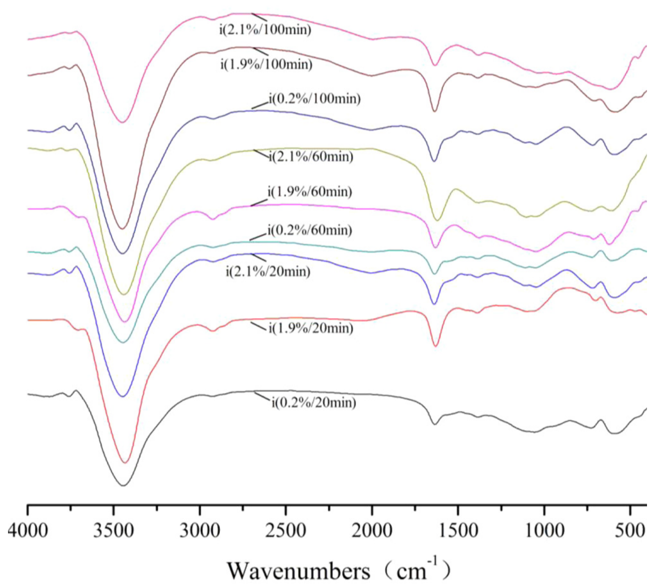

Figure 4 FT-IR spectra of acticarbon during adsorption of S solution.

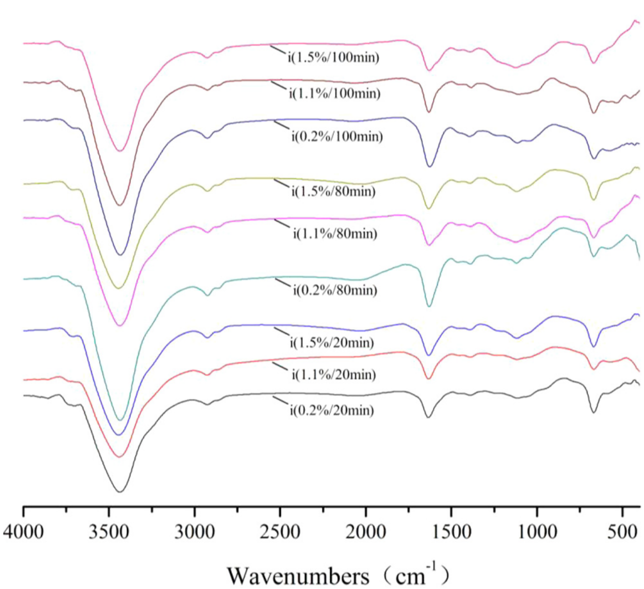

Figure 3 FT-IR spectra of acticarbon during adsorption of $Na_2S_2O_8$ solution.

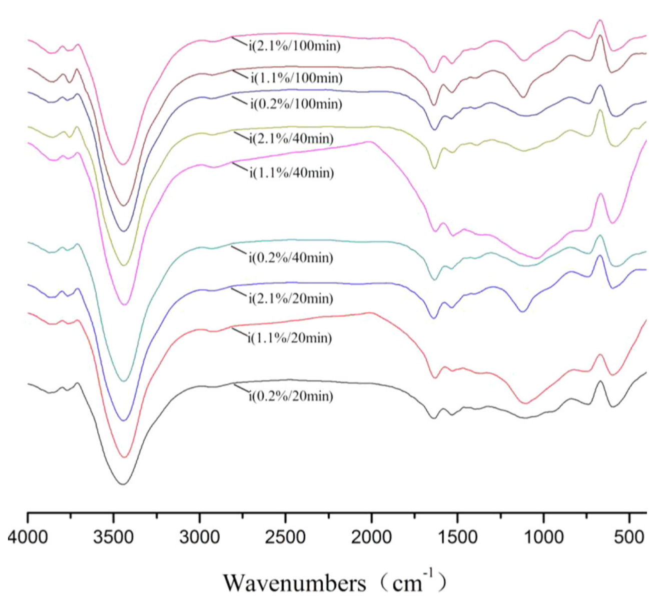

Figure 5 FT-IR spectra of acticarbon during adsorption of Na_2SO_3 solution.

capacities were 3.76 g/100 g, 1.75 g/100 g, 1.75 g/100 g, 2.49 g/100 g, 23.7 g/100 g, 18.5 g/100 g, 1 g/100 g, 0.5 g/100 g, 2.75 g/100 g for stir times of 20 min, 80 min, 120 min, respectively. When the concentrations of Na_2SO_4 were 11 g/1000 g, 19 g/1000 g, 21 g/1000 g, Na_2SO_4's adsorption capacities were 1.25 g/100 g, 3.52 g/100 g, 8.21 g/100 g, 0.75 g/100 g, 1.99 g/100 g, 1.75 g/100 g, 2.51 g/100 g, 2.26 g/100 g, 2.99 g/100 g for the stir time of 20 min, 60 min, 120 min, respectively. When the concentrations of $Na_2S_2O_8$ were 2 g/1000 g, 11 g/1000 g, 15 g/1000 g, $Na_2S_2O_8$'s adsorption capacities were 0.5 g/100 g, 8.25 g/100 g, 20.1 g/100 g, 1.79 g/100 g, 3.23 g/100 g, 12.7 g/100 g, 1.03 g/100 g, 2.23 g/100 g, 2.19 g/100 g for the stir time of 20 min, 80 min, 100 min, respectively. When the concentrations of S were 2 g/1000 g, 19 g/1000 g, 21 g/1000 g, S's adsorption capacities were 7.75 g/100 g, 37.3 g/100 g, 37.7 g/100 g, 4.52 g/100 g, 58.6 g/100 g, 80.3 g/100 g, 4.73 g/100 g, 11.5 g/100 g, 32.8 g/100 g for the stir time of 20 min, 60 min, 100 min, respectively. When the concentrations of Na_2SO_3 were 2 g/1000 g, 11 g/1000 g, 21 g/1000 g, Na_2SO_3's adsorption capacities were 0 g/100 g, 2.74 g/100 g, 1.25 g/100 g, 2.74 g/100 g, 2.74 g/100 g, 2.26 g/100 g, 1.75 g/100 g, 2.26 g/100 g, 4.26 g/100 g for the stir time of 20 min, 40 min, 100 min, respectively. It showed that adsorption capacity

Table 2 Groups of acticarbon during adsorption of $Fe_2(SO_4)_3$, Na_2SO_4, $Na_2S_2O_8$, S and Na_2SO_3 (%).

Kind	Peak (cm^{-1})	Adsorption time (min)/concentration (%)									Group
		20/0.5	20/0.9	20/2.1	80/0.5	80/0.9	80/2.1	120/0.5	120/0.9	120/2.1	
$Fe_2(SO_4)_3$	600	88.2	89.1	83.5	83.4	90.9	90.0	95.3	94.2	90.2	C—H
	1115	86.8	88.2	82.5	80.1	88.8	89.5	92.2	92.6	89.9	C—O stretch
	1390	87.1	89.5	84.2	83.4	88.8	90.0	91.2	91.9	90.5	CH_2 bend
	1630	84.7	84.2	82.0	82.6	86.1	86.6	86.8	87.2	87.3	C=O or C=C
	2925	88.8	89.5	88.6	88.2	88.8	88.6	87.9	88.8	89.0	—C—H stretch
	3435	76.1	73.4	74.6	72.6	76.4	77.4	79.1	73.5	76.4	O—H stretch
	3740	88.1	90.6	89.8	88.3	88.2	89.6	89.9	88.9	89.7	H_2O
	3850	88.1	90.6	89.7	88.2	88.3	90.2	90.0	89.5	90.1	S-S stretch
Na_2SO_4	Peak (cm^{-1})	20/1.1	20/1.9	20/2.1	60/1.1	60/1.9	60/2.1	120/1.1	120/1.9	120/2.1	Group
	600	85.8	86.1	87.5	83.9	83.2	84.2	86.5	85.5	90.1	C—H
	1115	84.5	84.7	85.6	81.3	83.6	80.2	84.4	82.8	88.1	C—O stretch
	1390	85.7	86.2	87.5	83.2	86.0	83.0	86.2	84.4	88.7	CH_2 bend
	1630	83.9	84.1	85.8	82.6	84.0	82.7	85.4	82.4	86.1	C=O or C=C
	2925	88.3	88.5	89.1	87.8	86.9	87.2	88.7	87.4	89.2	—C—H stretch
	3435	75.5	74.6	76.8	76.1	75.2	75.6	77.4	71.8	76.8	O—H stretch
	3740	88.5	88.1	89.0	87.9	89.5	87.9	89.2	87.9	88.5	H_2O
	3850	88.4	88.1	88.7	87.9	89.8	88.0	88.8	88.0	88.4	S-S stretch
$Na_2S_2O_8$	Peak (cm^{-1})	20/0.2	20/1.1	20/1.5	80/0.2	80/1.1	80/1.5	100/0.2	100/1.1	100/1.5	Group
	600	90.3	73.4	90.4	94.0	84.1	85.1	86.3	87.6	89.2	C—H
	1115	89.6	73.6	89.0	92.0	79.7	84.2	86.9	88.4	86.8	C—O stretch
	1390	89.9	73.8	90.0	91.9	83.2	85.9	87.8	89.3	88.7	CH_2 bend
	1630	86.9	70.9	86.5	86.1	82.7	85.3	83.4	85.9	86.2	C=O or C=C
	2925	88.6	71.4	88.9	87.7	87.8	88.8	87.3	88.8	87.9	—C—H stretch
	3435	77.3	60.9	76.4	71.6	74.7	79.2	72.4	73.9	75.9	O—H stretch
	3740	88.6	70.7	89.5	89.8	87.7	88.8	89.5	89.2	89.4	H_2O
	3850	89.5	71.0	90.1	90.2	87.7	88.7	89.7	89.9	89.9	S-S stretch
S	Peak (cm^{-1})	20/0.2	20/1.9	20/2.1	60/0.2	60/1.9	60/2.1	100/0.2	100/1.9	100/2.1	Group
	600	85.9	90.8	87.5	89.2	86.8	83.5	89.3	86.3	84.9	C—H
	1115	86.1	90.8	88.6	88.3	85.7	82.5	89.0	88.8	86.9	C—O stretch
	1390	87.6	90.6	89.5	89.2	86.9	84.2	89.8	89.7	88.2	CH_2 bend
	1630	86.7	86.8	86.7	87.5	85.6	82.0	86.6	85.9	87.1	C=O or C=C
	2925	89.7	88.6	91.1	90.4	88.7	88.6	88.8	92.3	92.0	—C—H stretch
	3435	80.5	75.0	77.2	80.6	78.1	74.6	74.8	74.2	81.4	O—H stretch
	3740	90.1	89.2	90.1	90.1	89.4	89.8	89.4	90.8	90.6	H_2O
	3850	89.8	89.9	89.8	89.9	90.0	89.7	90.0	90.5	90.4	S-S stretch
Na_2SO_3	Peak (cm^{-1})	20/0.2	20/1.1	20/2.1	40/0.2	40/1.1	40/2.1	100/0.2	100/1.1	100/2.1	Group
	600	87.6	83.8	89.5	87.6	82.0	88.1	89.6	88.9	88.9	C—H
	1115	86.4	80.8	86.7	87.4	78.7	87.5	89.7	86.1	87.4	C—O stretch
	1390	87.2	83.9	88.7	88.1	80.7	88.0	90.0	88.4	88.8	CH_2 bend
	1630	86.2	83.0	86.1	85.6	80.5	85.6	86.6	86.8	86.4	C=O or C=C
	2925	89.5	88.0	89.2	89.2	87.3	89.1	88.8	87.9	89.6	—C—H stretch
	3435	80.0	75.6	76.4	76.1	73.7	76.3	75.4	76.8	77.6	O—H stretch
	3740	89.2	88.5	88.4	88.9	87.7	89.0	89.1	89.4	88.3	H_2O
	3850	88.9	88.6	88.5	88.7	87.8	88.8	89.9	90.1	88.4	S-S stretch

changed at regularity difference. It might be because rapid stirring lead to a small amount of chemical medicine that was adsorbed by the acticarbon. The $Fe_2(SO_4)_3$'s optimal adsorption condition were the concentration was 9 g/1000 g and stir 80 min, the Na_2SO_4's optimal adsorption condition was the concentration of 21 g/1000 g and stir time of 20 min, the $Na_2S_2O_8$'s optimal adsorption condition was the concentration of 15 g/1000 g and stir time of 20 min, the S's optimal adsorption condition was the concentration of 21 g/1000 g and stir time of 60 min and the Na_2SO_3's optimal adsorption condition was the concentration of 21 g/1000 g and stir time of 100 min.

3.2. FT-IR analysis

FT-IR spectra were recorded to investigate the functional groups of acticarbon during adsorption of $Fe_2(SO_4)_3$, Na_2SO_4, $Na_2S_2O_8$, S, and Na_2SO_3.

Spectra of the samples were shown in Figs. 1–5. In the spectrum of adsorption, the S-S stretch, H_2O stretch, O—H stretch, —C—H stretch, C=O or C=C stretch, CH_2 bend, C—H, were observed at 3850 cm^{-1}, 3740 cm^{-1}, 3435 cm^{-1}, 2925 cm^{-1}, 1630 cm^{-1}, 1390 cm^{-1}, 1115 cm^{-1}, 600 cm^{-1}, respectively (listed in Table 2). For FT-IR spectra of $Fe_2(SO_4)_3$, the transmissivity of the peaks at 3850 cm^{-1}, 3740 cm^{-1}, 2925 cm^{-1} achieved the maximum for 20 min and the concentration was 9 g/1000 g, the transmissivity of the peaks at 3435 cm^{-1}, 600 cm^{-1} achieved the maximum for 120 min and the concentration was 5 g/1000 g, the transmissivity of the peaks at 1630 cm^{-1} achieved the maximum for 120 min and the concentration was 21 g/1000 g, the transmissivity of the peaks at 1390 cm^{-1}, 1115 cm^{-1} achieved the maximum for 120 min and the concentration was 9 g/1000 g.

For FT-IR spectra of Na_2SO_4, the transmissivity of the peaks at 3850 cm^{-1}, 3740 cm^{-1}, achieved the maximum for 60 min and the concentration was 11 g/1000 g, the transmissivity of the peaks at 3435 cm^{-1} achieved the maximum for 120 min and the concentration was 11 g/1000 g, the transmissivity of the peaks at 2925 cm^{-1}, 1630 cm^{-1}, 1390 cm^{-1}, 1115 cm^{-1}, 600 cm^{-1} achieved the maximum for 120 min and the concentration was 21 g/1000 g.

For FT-IR spectra of $Na_2S_2O_8$, the transmissivity of the peaks at 3850 cm^{-1}, 3740 cm^{-1}, 1390 cm^{-1}, 1115 cm^{-1}, 600 cm^{-1}, achieved the maximum for 80 min and the concentration was 2 g/1000 g, the transmissivity of the peaks at 3435 cm^{-1} achieved the maximum for 80 min and the concentration was 15 g/1000 g, the transmissivity of the peaks at 2925 cm^{-1} achieved the maximum for 20 min and the concentration was 15 g/1000 g, the transmissivity of the peaks at 1630 cm^{-1} achieved the maximum for 20 min and the concentration was 2 g/1000 g.

For FT-IR spectra of S, the transmissivity of the peaks at 3850 cm^{-1}, 3740 cm^{-1}, 2925 cm^{-1} achieved the maximum for 100 min and the concentration was 19 g/1000 g, the transmissivity of the peaks at 3435 cm^{-1} achieved the maximum for 100 min and the concentration was 21 g/1000 g, the transmissivity of the peaks at 1630 cm^{-1} achieved the maximum for 60 min and the concentration was 2 g/1000 g, the transmissivity of the peaks at 1390 cm^{-1}, 1115 cm^{-1}, 600 cm^{-1} achieved the maximum for 20 min and the concentration was 19 g/1000 g.

For FT-IR spectra of Na_2SO_3, the transmissivity of the peaks at 3850 cm^{-1}, 3740 cm^{-1} achieved the maximum for 100 min and the concentration was 11 g/1000 g, the transmissivity of the peaks at 3435 cm^{-1} achieved the maximum for 20 min and the concentration was 2 g/1000 g, the transmissivity of the peaks at 2925 cm^{-1} achieved the maximum for 100 min and the concentration was 21 g/1000 g, the transmissivity of the peaks at 1630 cm^{-1}1390 cm^{-1}, 1115 cm^{-1}, 600 cm^{-1} achieved the maximum for 100 min and the concentration was 2 g/1000 g.

4. Conclusion

As we can see from the above methods, $Fe_2(SO_4)_3$'s, Na_2SO_4's, $Na_2S_2O_8$'s, S's, and Na_2SO_3's adsorption capacity were different for several stir times and several concentrations, respectively. The $Fe_2(SO_4)_3$'s optimal adsorption condition was the concentration was 9 g/1000 g and stir time of 80 min, the Na_2SO_4's optimal adsorption condition was the concentration was 21 g/1000 g and stir 20 min, the $Na_2S_2O_8$'s optimal adsorption condition was the concentration of 15 g/1000 g and stir time of 20 min, the S's optimal adsorption condition was the concentration was 21 g/1000 g and stir time of 60 min and the Na_2SO_3's optimal adsorption condition were the concentration of 21 g/1000 g and stir time of 100 min.

FT-IR spectra showed that acticarbon had the eight characteristic absorption band. And the S-S stretch, H_2O stretch, O—H stretch, —C—H stretch, C=O or C=C stretch, CH_2 bend, C—H, were observed at 3850 cm^{-1}, 3740 cm^{-1}, 3435 cm^{-1}, 2925 cm^{-1}, 1630 cm^{-1}, 1390 cm^{-1}, 1115 cm^{-1}, 600 cm^{-1}, respectively. For FT-IR spectra of $Fe_2(SO_4)_3$, the transmissivity of the peaks at 3850 cm^{-1}, 3740 cm^{-1}, 2925 cm^{-1} achieved the maximum for 20 min and the concentration was 9 g/1000 g. For FT-IR spectra of Na_2SO_4, the transmissivity of the peaks at 2925 cm^{-1}, 1630 cm^{-1}, 1390 cm^{-1}, 1115 cm^{-1}, 600 cm^{-1} achieved the maximum for 120 min and the concentration was 21 g/1000 g. For FT-IR spectra of $Na_2S_2O_8$, the transmissivity of the peaks at 3850 cm^{-1}, 3740 cm^{-1}, 1390 cm^{-1}, 1115 cm^{-1}, 600 cm^{-1}, achieved the maximum for 80 min and the concentration was 2 g/1000 g. For FT-IR spectra of S, the transmissivity of the peaks at 3850 cm^{-1}, 3740 cm^{-1}, 2925 cm^{-1} achieved the maximum for 100 min and the concentration was 19 g/1000 g, the transmissivity of the peaks at 1390 cm^{-1}, 1115 cm^{-1}, 600 cm^{-1} achieved the maximum for 20 min and the concentration was 19 g/1000 g. For FT-IR spectra of Na_2SO_3, the transmissivity of the peaks at 1630 cm^{-1}, 1390 cm^{-1}, 1115 cm^{-1}, 600 cm^{-1} achieved the maximum for 100 min and the concentration was 2 g/1000 g. In these states, the number of the transmissivity of the maximum peaks is the largest.

Acknowledgment

This work was financially supported by the National 948 Plan (2014-4-38).

References

Ahmadpour, A., Do, D.D., 1996. The preparation of activated carbon from coal by chemical and physical activation. Carbon 34 (4), 471–479.

Chai, X.W., Wang, Y.N., Liao, X.P., et al, 2010. Leather on the determination of ammonia nitrogen in wastewater and source analysis. China Leather 17 (3), 332–335.

Chandra, T.C., Mirna, M.M., Sunarso, J., et al, 2009. Activated carbon from durian shell: Preparation and characterization. J. Taiwan Inst. Chem. Eng. 40 (4), 457–462.

Cui, L., Peng, W.X., Sun, Z.J., 2014. Weibull statistical analysis of tensile strength of vascular bundle in inner layer of moso bambooculm in molecular parasitology and vector biology. Pak. J. Pharm. Sci. 27 (4), 1083–1087.

Ding, L.P., Bhatia, Liu, K., S.K., Liu, K., 2002. Kinetics of adsorption on activated carbon: Application of heterogeneous vacancy solution theory. Chem. Eng. Sci. 57 (18), 3909–3928.

He, Y., Zhao, Y.C., Zhou, G.M., 2008. Journal of the high concentration of ammonia nitrogen wastewater denitrification technology. Ind. Water Treat. 28 (1), 1–4.

Ikuo, A., Tomoko, F., Jun, M., et al, 2001. Preparation of carbonaceous adsorbents for removal of chloroform from drinking water. Carbon 39, 1069–1073.

Jumasiah, A., Chuah, T.G., Gimbon, J., et al, 2005. Adsorption of basic dye onto palm kernel shell activated carbon: Sorption equilibrium and kinetics studies. Desalination 186 (1/3), 57–64.

Kei, M., Toshitatsu, M., Yasuo, H., 1994. Removal of nitrate-nitrogen from drinking water using bamboo powder charcoal. Bioresour. Technol. 95, 255.

Lin, Z., Ge, S.B., Li, D.L., Peng, W.X., 2015. Structure Characteristics of Acidic Pretreated Fiber and Self-bind Bio-boards for Public Health. J. Pure Appl. Microbiol. 9, 221–226.

Liu, Q.M., Luo, Y.S., Yin, S.P., et al, 2008. Liquid rheology study on refined rapeseed oil. J. Cent. South Univ. Technol. 15, 525–528.

Mao, Y.T., Liu, Z.Q., Qiao, X.Y., et al, 2000. The analysis and research of the aquatic products processing wastewater ammonia nitrogen removing abnormal. The Prevent. Control Environ. Pollut. 31 (8), 101–106.

Masakazu, K., Shogo, T., Hyun-Min, K., et al, 2003. Preparation of antibacterial silver-doped silica glass microspheres N. J. Biomed. Mater. Res. 66, 266.

Milena, I., David, L., Sandrine, L., Christine, J., 2003. Immobilization of silver in polypyrrole/polyanion composite coatings: preparation, characterization, and antibacterial activity. Langmuir 19, 8971–8979.

Parag, A.P., Bhanu, R., 2013. The Ft-Ir spectrometric studies of vibrational bands of semecarpus anacardium Linn.F. leaf, stem powder and extracts. Asian J. Pharm. Clin. Res. 6, 159–198.

Peng, W.X., Le, C., 2012. Crystal structure of 3-(3-bromophenyl)-4-(3,5-dichloro-phenylamino)furan-2(5H)-one $C_{16}H_{10}BrCl_2NO_2$. Z. Kristallogr. – New Cryst. Struct. 227 (2), 267–268.

Peng, W.X., Wang, L.S., Wu, F.J., Xu, Q., 2011. 3-(4-Bromophenyl)-4-(4-hydroxyanilino)furan-2(5H)-one. Acta Crystallogr. Sect. E – Struct. Rep. Online 67. O2329-U206.

Peng, W.X., Wu, F.J., Wang, L.S., Xu, Q., 2012. Crystal structure of 3-(4-bromophenyl)-4-(4-chlorophenylamino)furan-2(5H)-one C16H11BrClNO2. Z. Kristallogr. – New Cryst. Struct. 227 (1), 61–62.

Peng, W.X., Lin, Z., Chang, J.B., Gu, F.L., Zhu, X.W., 2013a. Biomedical Molecular Characteristics of Ybsj Extractives from Illicium Verumfruit. Biotechnol. Biotechnol. Equip. 27 (6), 4311–4316.

Peng, W.X., Wang, L.S., Lin, Z., et al, 2013b. Identification and Chemical Bond Characterization of Wood Extractives in Three Species of Eucalyptus Biomass. J. Pure Appl. Microbiol. 7, 67–73.

Peng, W.X., Wang, L.S., Zhang, M.L., Lin, Z., 2013c. Molecule characteristics of eucalyptus hemicelluloses for medical microbiology. J. Pure Appl. Microbiol. 7 (2), 1345–1349.

Peng, W.X., Ge, S.B., Li, D.L., Mo, B., Daochun, Q., Ohkoshi, M., 2014a. Molecular basis of antibacterial activities in extracts of Eucommia ulmoides wood. Pak. J. Pharm. Sci. 27 (6), 2133–2138.

Peng, W.X., Wang, L.S., Zhang, M.L., Lin, Z., 2014b. Separation characteristics of lignin from Eucalyptus camaldulensis lignincelluloses for biomedical cellulose. Pak. J. Pharm. Sci. 27, 723–728.

Peng, W.X., Lin, Z., Chen, H., Wu, J.G., 2015. Biochemical Group Characteristics of Self-Bonded Boards During Acidic Oxidation for Public Health. J. Pure Appl. Microbiol. 9, 307–311.

Pu, H.Z., Jiang, J.C., 2005. Modified activated carbon materials used for flue gas desulfurization. Forest Chem. Commun. 39 (5), 29–33.

Qi, H.C., Peng, W.X., Wu, Y.Q., Wu, S.B., Xu, G.J., 2012. Effects of alkaline extraction on micro/nano particles of eucalyptus camaldulensis biology. J. Comput. Theor. Nanosci. 9 (9), 1525–1528.

Schindler, D.W., 1988. Effects of acid rain on freshwater ecosystems. Science 239 (4836), 149–157.

Sun, Y.C., Lin, Z., Peng, W.X., et al, 2014. Chemical changes of raw materials and manufactured binderless boards during hot pressing: lignin isolation and characterization. Bioresources 9 (1), 1055–1071.

Wang, Y.X., 2004. Journal of the activated carbon desulfurization denitration technology. Power Syst. Eng. 20 (6), 41–42.

Wang, J.X., Wen, L.X., Wang, Z.H., Chen, J.F., 2006. Immobilization of silver on hollow silica nanospheres and nanotubes and their antibacterial effects. Mater. Chem. Phys. 96 (1), 90–97.

Wang, T.H., Tan, S.X., Liang, C.H., 2009. Preparation and characterization of activated carbon from wood via microwave-induced $ZnCl_2$ activation. Carbon 47 (7), 1880–1883.

Wang, Z.Z., Lv, P., Hu, Y., Hu, K.L., 2009. Thermal degradation study of intumescent flame retardants by TG and FTIR: melamine phosphate and its mixture with pentaerythritol. J. Anal. Appl. Pyrolysis 86, 207–214.

Wang, L.S., Peng, W.X., Zhang, M.L., Lin, Z., 2013. Separation characteristics of lignin from eucalyptus lignincellulose for medicinal biocellulose preparation. J. Pure Appl. Microbiol. 7, 59–66.

Xiao, Z.P., Peng, Z.Y., Dong, J.J., et al, 2013. Synthesis molecular docking and kinetic properties of beta-hydroxy-beta-phenylpropionyl- hydroxamic acids as Helicobacter pylori urease inhibitors. Eur. J. Med. Chem. 68, 212–221.

Xue, Q., Peng, W.X., Ohkoshi, M., 2014. Molecular bonding characteristics of Self-plasticized bamboo composites. Pak. J. Pharm. Sci. 27, 975–982.

Yu, G.X., Lu, S.X., Chen, H., et al, 2005. Diesel fuel desulfurization with hydrogen peroxide promoted by formic acid and catalyzed by activated carbon. Carbon 43 (11), 2285–2294.

Yuan, C.S., Lin, H.Y., Wu, C.H., et al, 2004. Preparation of sulfurized powdered activated carbon from waste tires using an innovative compositive impregnation process. J. Air Waste Manag. Assoc. 54 (7), 862–870.

Zhang, D.Q., Chen, S.M., Peng, W.X., et al, 2008. Rheology study of supercritically extracted tea-oil. J. Cent. South Univ. Technol. 15, 506–508.

Zhang, H.O., Yan, Y., Yang, L.C., 2010. Preparation of activated carbon from sawdust by zinc chloride activation. Adsorption 16 (3), 161–166.

Zhou, P.Y., Qian, Q.R., Xiao, L.R., et al, 2007. Preparation of polyvinyl chloride (PVC) plastic waste activated carbon fiber. Plast. Ind. 10 (1), 34–37.